ELSEVIER

Catalysis Today 49 (1999) 285–292

CATALYSIS TODAY

Pore size and crystal size effects on the selective hydroisomerisation of C_8 paraffins over Pt–Pd/SAPO-11, Pt–Pd/SAPO-41 bifunctional catalysts

P. Mériaudeau*, Vu.A. Tuan, G. Sapaly, Vu.T. Nghiem, C. Naccache

Institut de Recherches sur la Catalyse, CNRS 2, Av. Einstein, 69626 Villeurbanne Cedex, France

Abstract

The hydroconversion of *n*-octane over bifunctional Pt–Pd/SAPO-11 and Pt–Pd/SAPO-41 catalysts was studied. High selectivity, 90% towards isomerisation, was observed even at high conversion. SAPO-41 was found slightly more selective than SAPO-11. The grain sizes have a profound effect on conversion, small grains were more active than large grains, but had almost no significant effect on the selectivity and product distributions. It was concluded that the reaction of *n*-octane occurs in the SAPO's channels but the molecules did not penetrate too far in the channels. Restricted transition shape selectivity at the SAPO pore mouth is responsible for the product distributions observed. These hypotheses were further supported by the study of monoethyl heptane isomers and of dimethyl hexane isomers. Pore size effects and particle size effects indicate that it is highly probable that the reactions occurred in the channels not too deep from the surface. Restricted transition-state selectivity was the main factor governing the extent of methyl debranching in branched C_8 isomers. A relatively small difference in the size of the channels resulted in a significant difference in the constraint exerted by the pore dimension, smaller the pore dimension higher the tendency for the catalyst to form monobranched isomer with the methyl at terminal position.

Also high selectivity for debranching the methyl branched C_8 isomers is obtained with these medium monodimensional pore SAPO materials. Small-grain molecular sieves were more effective than large-grain samples particularly if amount of acid sites on the outer surface is small.

Keywords: Hydroisomerisation; Pore size; Crystal size; SAPO

1. Introduction

Normal paraffins react over bifunctional catalysts via consecutive reactions: dehydrogenation into olefins and isomerisation to monobranched, dibranched, multibranched olefins, followed by a very fast cracking of the multibranched isomers and rehydrogenation. High selectivity towards hydroisomerisation is attainable by preventing the occurrence of mutlibranched paraffins. Platinum (palladium) supported on narrow tubular-pore molecular sieves, ZSM-22 [1] SAPO-11 [2] showed very high efficiency for the selective hydroisomerisation of long chain paraffins. The unidimensional pore structure and the narrow size of the 10-membered ring channels (0.44 nm×0.55 nm diameter ZSM-22 and 0.39 nm×0.63 nm diameter SAPO-11) are responsible for the high isomerisation selectivity. A new process for lube dewaxing based on SAPO-11 has been developed [3]. In a recent work we have shown that Pt/SAPO-31, and Pt/SAPO-41 having

*Corresponding author. Tel.: +33-0-472445342.

0920-5861/99/$ – see front matter
PII: S0920-5861(98)00435-0

unidimensional pore structures and narrow 10-membered ring channels (0.43 nm×0.7 nm diameter for SAPO-41) are also selective for the hydroisomerisation of *n*-octane [4]. The isomerised products contained a very large fraction of monobranched isomers (2-methyl C_7, 3-methyl C_7) being favoured. The preference for terminal branching was also encountered in the distribution of the dimethyl branched isomers. Restricted transition-state shape selectivity was invoked to explain the preferential formation of terminal monobranched alkanes [2,5,6]. Product-shape selectivity was also considered as a possible explanation, the diffusion of 2-methylalkane being faster than that of the other monomethyl isomers [5]. These interpretations were questioned according to molecular graphics study. Molecular graphics concluded that protonated cyclopropane intermediates, as well methylalkenes cannot be accommodated inside ZSM-22 pores [7]. The authors suggested that catalysis occurred at the ''pore mouth''. In addition, the concept of *key lock* catalysis was introduced to explain the product distribution within the multibranched isomers [8].

Therefore it is important to examine whether the hydroisomerisation selectivity of narrow tubular pore molecular sieves can be explained exclusively with one of the above shape selective concepts or if simultaneously transition-state, product diffusion and pore-mouth shape selective catalysis contribute to the overall product distribution. This study was specifically intended to address the above concerns. Our approach consisted to compare reaction rate and product distribution in relation with the diameter of the unidimensional pores and also in relation with the crystal sizes. Hydroconversion of various C_8 paraffin isomers with increasing molecular diameters were reacted over SAPO-41 (0.43 nm×0.70 nm diameter) and SAPO-11 (0.39 nm×0.63 nm) supporting Pt–Pd. For each material the study was made over large crystals and over small crystals.

2. Experimental

SAPO-11 [9] and SAPO-41 [10] were synthesised following the procedures published earlier. These procedures have led to materials formed by relatively large crystals (Samples A). By adding to the classical synthesis solutions a surfactant, dodecylamine in hexanol, a series of SAPO-11 and SAPO-41 composed of small crystals were formed (Samples B). The synthesis procedures, gel compositions and properties of these solids are given in a forthcoming paper [11]. The template, dipropylamine, was removed by calcination in air at 873 K. X-ray diffractograms indicated that the materials were highly crystalline. The grain sizes measured by scanning electron microscopy were, respectively, 1–1.5 μm for SAPO-11 (Sample A) and 0.1–0.2 μm SAPO-11 (B). SAPO-41 (A) showed grains with 2–5 μm diameter while SAPO-41 (B) grains were smaller, 0.2–0.5 μm in diameter. The Bronsted acidity of these samples was determined by TPD of absorbed ammonia, and by the relative intensity of the IR band at 3630 cm^{-1} due to acidic OH groups. The results which will be presented in [11] indicated that the Bronsted acidity of SAPO-11 (A) is almost identical to that of SAPO-11 (B). Similar observations were made concerning the acidity of samples A and B, SAPO-41.

The bifunctional catalysts were obtained by impregnating the SAPOs samples with Pt and Pd tetramine chloride solutions. The impregnated solids were then calcined in air at 673 K and finally reduced in H_2 at 773 K.

The Pt and Pd contents were adjusted such that the metal loadings were 0.6 wt% Pt and 1.2 wt% Pd.

2.1. Catalytic reaction

Hydroconversion measurements were carried out at atmospheric pressure in a continuous flow fixed-bed microreactor, loaded with 0.1 g of the catalyst powder. The temperature of the catalyst bed was 523 K. The reactant gas mixture of the alkane and H_2 (H_2:HC=60) was fed to the reactor, the flow rate being dosed by electronic mass flow controllers (Brooks). The hydrocarbon conversion was monitored by adjusting the flow rate at the desirable value. The product gas-mixtures were analysed using a gas chromatograph equipped with a Pona capillary column (Altech France) for C_8 isomers. The cracked products were analysed with a second chromatograph equipped with an unibead 3S Column. *n*-Octane, 2 Me-heptane ($2MeC_7$), $3MeC_7$, $4MeC_7$, 2,5 dimethylhexane (2,5 $dMeC_6$), and 2,2 trimethylpentane (2,2,4 TMP) from Aldrich were used without further purification.

3. Results

The distribution of the cracked products is shown in Fig. 1 for SAPO-41. Identical curves were obtained with SAPO-11 [11]. The results are given at 32% and ~80% conversion of *n*-C_8, the reaction temperature was 523 K. Fig. 1 indicates that the C_1, C_2 cracking fractions were relatively small which suggests that *n*-C_8 hydrogenolysis on the metal Pt–Pd is negligible. In addition, symmetrical distribution around the C_4 fraction was obtained for the cracked products. Finally the results showed that *n*-octane conversion varied like the inverse of the hydrogen pressure. It was concluded that the four samples possessed well-balanced metallic and acid functions resulting in a true bifunctional mechanism.

In Table 1 are compared the results of the *n*-octane reaction over the four samples. The sample activities are given by the product: conversion×WHSV. The activity of small crystals (SAPO-11 and SAPO-41) for *n*-octane was always higher than that of large crystals. Small crystal SAPO-11 sample was approximately 14 times more active than large crystal sample, while small crystal SAPO-41 is only 4.6 times more active than large crystal sample. In general, the selectivity towards isomerisation is slightly higher over SAPO-41 samples as shown in Table 1. However, it can be seen from Table 1 that the crystal sizes have no significant influence on the product distributions. The selectivity to monomethylheptanes is considerably higher than that to dimethylhexanes. The molecular ratio $2MeC_7$/$3MeC_7$ was around 1.4 for the four samples, the preferential formation of $2MeC_7$ among the other monomethylheptanes being slightly reinforced over SAPO-11 catalysts.

Table 1
Transformation of *n*-octane over different solids: crystal size effect

	Crystal size			
	SAPO-11		SAPO-41	
	Large	Small	Large	Small
α[a] WHSV[b]	11.4	162	28.0	129
α	10.4	7.8	6.8	9.3
S^d_{crack} (%)	4.3	5.4	0.5	1.1
$S^e_{isom.}$ (%)	95.7	94.6	99.5	98.9
$2MeC_7$(%)[c]	58.7	56.9	55.8	56.4
$3MeC_7$(%)[c]	38.5	38.0	41.9	39.4

[a]α: Conversion (%).
[b]WHSV: weight hour space velocity.
[c]$2MeC_7$ and $3MeC_7$ among isomerised products.
[d]Selectivity into cracking.
[e]Selectivity into isomerisation.

Table 2 shows the results of the reaction of 2,2,4 TMP at 523 K over the four samples. The relative activity (α×WHSV) and the product selectivity are shown. 2,2,4 TMP molecule is too large to penetrate the pores of SAPO-11 and SAPO-41. Consequently the reaction occurred with the Bronsted acid sites located at the external surface of the grains. Table 2 indicates that the outer surface of small crystal SAPO-11 is twice as more active than that of large crystals.

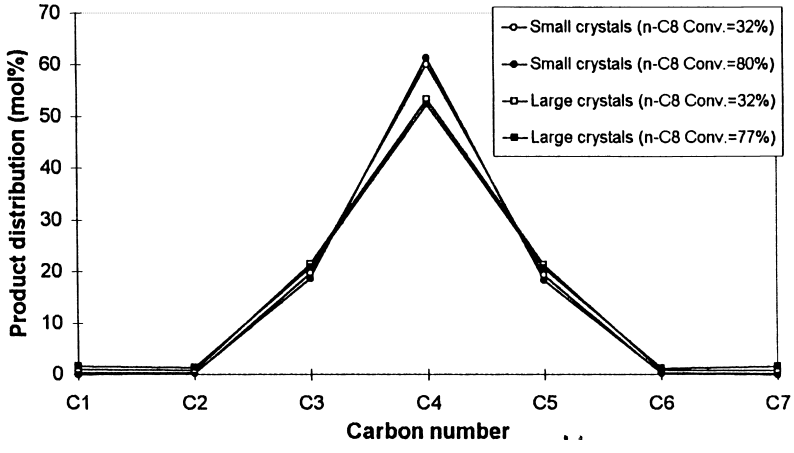

Fig. 1. Hydroconversion of *n*-octane. Distribution of cracked products over different solids.

Table 2
Transformation of 2,2,4 TMC_5 over different solids: crystal size effect

	Crystal size			
	SAPO-11		SAPO-41	
	Large	Small	Large	Small
α[a] WHSV[b]	16.5	29.3	1.3	32.9
α	7.5	3.5	1.6	4.0
$S_{isom.}$ (%)	14.0	20.5	17.0	23.0
$S_{cracking}$ (%)	86.0	79.5	83.0	77
S[c]iC_4	99.2	99.1	98.4	99.8

[a]α: Conversion (%).
[b]WHSV in h^{-1}.
[c]Percentage of isobutane among the cracking fraction.

By contrast in the case of SAPO-41 samples the external surface of small grains was almost 25 times more active than that of large grains. We believe that the difference in the acid site distribution, between surface and bulk shown by SAPO-11 in comparison with SAPO-41, is the result of the synthesis procedures used in this work, and not an intrinsic property attached with SAPO-11 and SAPO-41. The dominant reaction occurring was hydrocracking via β-scission of 2,2,4 TMP^+ as indicated by the preferential production of isobutane.

The relative reaction rates ($\alpha \times$WHSV) observed for the reaction of $2MeC_7$, $3MeC_7$, $4MeC_7$, 2,5 $dMeC_6$ and 2,4 $dMeC_6$ are listed in Table 3. Similarly to what was observed with *n*-octane and 2,2,4 TMP, small crystals were always more active than large crystals. In the case of methyl-heptane reactions, the effect of crystal size of the reaction rate was more important with SAPO-11 (10–15 times) than with SAPO-41 (2–3 times). The same observation was made for the reaction of dimethyl hexanes.

Table 3
Transformation of MeC_7 and $dMeC_6$ over different solids: crystal size effect

Reactant	Crystal size			
	SAPO-11		SAPO-41	
	Large	Small	Large	Small
$2MeC_7$	26	215	98	289
$3MeC_7$	20	217	97	220
$4MeC_7$	19	206	88	215
2,5 $dMeC_6$	3.5	42.7	10.2	37.8
2,4 $dMeC_6$	3.1	38.2	9.1	33.2

Relative rates (a.u) $\alpha \times$WHSV; α being conversion, WHSV in h^{-1}, α<10%.

The distribution of products formed from methylheptanes and dimethylhexanes are given in Tables 4 and 5, at low degree of conversion. It can be seen that the cracking reaction for all the C_8 isomers was limited and played a minor role in the feed conversion. The cracked products were distributed symmetrical around C_4, which proved again the well balanced bifunctional character of the catalyst. Starting from monomethylheptanes for all four samples methylbranching reaction to form dimethylhexanes occurred to less extent than methyl shift without changing the degree of branching, as well than that of methyl debranching to form *n*-octane. Similarly to what has been observed with *n*-octane, the dibranched C_8 isomers contained principally 2,5 and 2,4 $dMeC_6$ with a strong preference for 2,5 $dMeC_6$ (Table 4). The values for the molar ratio 2,5 $dMeC_6$/2,4 $dMeC_6$ are approximately 2, much larger than the thermodynamic value (2,5 $dMeC_6$/2,4 $dMeC_6$=1.1 at 523 K).

Among dimethylhexane isomers, SAPO-11 and SAPO-41 form preferentially terminal methyl isomers. However, it can be seen in Table 4 that the molar ratio 2,5 $dMeC_6$/2,4 $dMeC_6$ hardly changed with the crystal sizes and also no difference between SAPO-11 and SAPO-41 existed towards the preferential formation of 2,5 $dMeC_6$. Hence one can conclude that the preferential formation of terminal dimethylhexane was not controlled by product-shape selectivity involving differences in the rate of diffusion.

Table 4 indicates that at low conversion the major reactions occurring for MeC_7 isomers were 1,2 methyl shift without changing the degree of branching and methyl debranching to form *n*-octane. Also the striking results were that whatever was the starting MeC_7 isomer, *n*-octane, from debranching reaction, was always formed in a substantial amount. Analysis of the results presented in Table 5 shows that the cracking of $dMeC_6$ did not occur appreciably, the main reaction path being isomerisation. It is remarkable that the rearrangements of the $dMeC_6$ skeleton occurred preferentially towards the increase of the carbon skeleton of the C_8 paraffin and the subsequent formation of monomethylheptanes and *n*-octane.

Table 4
Hydroisomerisation of MeC_7 isomers over SAPO-11 and SAPO-41 (small and large crystals)

Reactant	Large crystals			Small crystals		
	$2MeC_7$	$3MeC_7$	$4MeC_7$	$2MeC_7$	$3MeC_7$	$4MeC_7$
SAPO-11						
S_{crack} (%)	3.0	2.4	2.9	3.9	3.3	3.1
$S_{isom.}$ (%)	97.0	97.6	97.1	96	96.7	96.9
$dMeC_6$ (%)	8.6	3.8	4.2	8.6	4.7	2.0
$2MeC_7$ (%)	–	58.8	[a]	–	55.9	[a]
$3MeC_7$ (%)	68.9	–	87.8	59.3	–	90.5
$4MeC_7$ (%)	[a]	22.5	–	[a]	11.0	–
n-C_8	22.5	14.9	8.0	32.2	28.4	7.5
SAPO-41						
S_{crack} (%)	0.7	0.1	0.3	1.0	0.4	0.6
$S_{isom.}$ (%)	99.3	99.9	99.7	99.0	99.6	99.4
$dMeC_6$ (%)	9.6	2.6	1.9	9.2	4.7	3.3
$2MeC_7$ (%)	–	58.0	[a]	–	53.5	[a]
$3MeC_7$ (%)	73.0	–	90.5	63.0	–	81.1
$4MeC_7$ (%)	[a]	26.8	–	[a]	19.7	–
n-C_8 (%)	17.4	12.5	7.6	27.8	22.0	15.6

[a] $2MeC_7$ and $4MeC_7$ are not discriminated when one of the two compounds is in large excess compared to the other.

Table 5
Hydroisomerisation of 2,4 $dMeC_6$ and 2,5 dMC_6 over small and large crystals (SAPO-11 and SAPO-41), α<10%

Reactant	Large crystal		Small crystal	
	2,4 $dMeC_6$	2,5 $deMC_6$	2,4 $dMeC_6$	2,5 $dMeC_6$
SAPO-11				
S_{crack} (%)	21.4	14.8	7.0	9.4
$S_{isom.}$ (%)	78.6	85.2	93.0	90.6
MeC_7 (%)	26.0	65.9	42.6	67.7
n-C_8	1.6	9.2	8.1	13.7
2,2 $dMeC_6$ (%)	8.7	2.6	3.8	1.5
3,3 $dMeC_6$ (%)	–	–	–	–
2,3 $dMeC_6$ (%)	44.2	10.8	30.9	6.0
3,4 $dMeC_6$ (%)	19.4	11.5	14.6	11.1
SAPO-41				
Sel. craq.	1.5	1.8	2.7	2.8
Sel. isom.	98.5	98.2	97.3	97.2
MeC_7 (%)	48.2	77.3	45.9	70.3
n-C_8 (%)	6.8	10.1	7.6	13.2
2,2 $dMeC_6$ (%)	0.8	–	3.2	0.4
3,3 $dMeC_6$ (%)	1.7	–	1.4	0.1
2,3 $dMeC_6$ (%)	26.3	4.1	29.2	5.2
3,4 $dMeC_6$ (%)	16.2	8.5	12.8	10.8

Note: 2,4 $dMeC_6$ and 2,5 $dMeC_6$ are not discriminated if one of two compounds is in large excess compared to the other.

4. Discussion

In agreement with previous works [2,4] the results presented in this study clearly indicate that small pore monodimensional channel SAPO-11 are highly selective for the hydroisomerisation of long chain alkanes. SAPO-41 apparently is slightly more selective than SAPO-11 probably due, as suggested in [4], to a slightly larger pore dimension as compared to SAPO-11. The larger pore dimensions in SAPO-41 renders the diffusion of methyl branched isomers less constraint than in the case within the channels of SAPO-11. The residence time of the branched paraffins in the pores of SAPO-41 is less than in SAPO-11 and thus less cracking occurs. In conclusion, it is suggested that the high selectivity of SAPO-41 (as well of SAPO-11) towards hydroisomerisation of *n*-octane into monobranched methyl heptanes is due to the difficult and highly constraint formation of dimethylhexane isomers as a consequence of the pore sizes, and to the facile diffusion out of the channels of the monobranched methyl-isomers. The extent of secondary reactions, ultimately to multibranched C_8 and cracking, is hence considerably lowered.

Small crystal SAPO-11 and SAPO-41 bifunctional catalysts showed almost the same activity in the reaction of 2,2,4 TMP. Cracking was the main reaction in agreement with the tertiary–tertiary carbenium ion mechanism involved in the β-scission of 2,2,4 TMP^+, more favourable that the tertiary–secondary mechanism for isomerisation. By contrast, large crystal SAPO-41 was less active than SAPO-11 for 2,2,4 TMP.

In general, the intracrystalline surface of molecular sieve is almost of two order magnitude larger than that of the external grain surface. It results that in the absence of diffusion limitation, the contribution of the grain surface to the catalytic reaction is negligible. By contrast the contribution of the internal surface becomes negligible when the molecule is too large to enter the pore. When the reactant and/or the products have critical diameters close to those of the molecular sieve pores the respective contributions of the catalytic reaction occurring on the outer surface and in the intracrystalline void can be determined by changing the crystal sizes. The results on the reaction of 2,2,4 TMP have indicated that the outer surface of small crystal SAPO-11 is approximately 2 times more active than that of large crystal sample. By contrast in *n*-octane reaction small crystal SAPO-11 was almost 14 times more active than large crystal. These results exclude the possibility that the reaction of *n*-octane occurred only on the outer surface of the grains. The change in the reaction rate with the crystal sizes indicates that the intracrystalline reaction of *n*-octane over SAPO-11 obeys to shape-selective constraint. In general, when the reaction rate increases as the crystal size decreases, and if further it was excluded that the reaction occurs on the surface grains, it is concluded that the rate of diffusion controls the rate of reaction. The observed rate will be proportional to $\sqrt{1/d}$, d being the diameter of the crystal. It is clear from the results given in Table 1 that this relation is not obeyed since the ratio of the rates measured on small and on large SAPO-11 crystals is 14 while the ratio of the square root of d is 3.1. The same conclusions are reached by analyzing the results of *n*-octane reaction over SAPO-41. It is clear that neither grain surface reaction nor intracrystalline diffusion can explain significatively the results. Restricted transition-state selectivity is probably the best explanation as already proposed in [1,2]. To the effect of restricted transition-state shape selectivity one should add the concept of pore-mouth catalysis since the reaction rate of *n*-octane do change with the crystal sizes. Indeed if the restricted transition-state intermediates are formed only at the pore mouth at a short distance from the surface-intracrystalline boundary, it is conceivable that the number of pore mouths (hence the activity) will increase with the outer surface of the crystals (proportional to $1/d$). The length of the ''pore mouth'' which would intervene in the catalytic reaction will probably depend on the diffusion rate of the intermediates and/or reactant-products but not on the crystal sizes. As a consequence, the important factors controlling the efficiency of the catalyst for the hydroisomerisation reaction will be the dimensions of the pores and the dimensions of the crystals.

The isomerisation of linear alkyl carbenium ions involves the formation of protonated cyclopropyl carbenium ion intermediates. PCP ring opening forms monobranched alkyl carbenium ion. This type of rearrangement is slower than the rearrangement by methyl shift occurring in monobranched alkyl carbenium ion. *n*-Octyl carbenium ions formed by protonation of *n*-octene in the intracrystalline void of

SAPO-11 and 41 at the pore mouth rearrange into alkyl protonated cyclopropyl intermediates. The PCP ring can probably accommodate within the pore of SAPO-11 and SAPO-41, the kinetic diameter of cyclopropane is 0.42 nm. It was suggested that the formation of the more central PCP intermediate from *n*-decane in H-ZSM-5 is hindered [5]. Table 1 shows that SAPO-11 and SAPO-41 favoured the formation of $2MeC_7$ above the thermodynamic equilibrium ($2MeC_7/3MeC_7$=0.9 at 523 K at equilibrium). Furthermore, Table 1 indicates that the observed values for the molecular ratio $2MeC_7/3MeC_7$ did not change with the crystal sizes, the value is, respectively, 1.5 for SAPO-11 and 1.33 for SAPO-41 at 7–10% *n*-C_8 conversion. It follows from the foregoing that over unidimensional small pore SAPO-11 and SAPO-41 the hydroisomerisation of *n*-octane to produce preferentially terminal monobranched methyl heptane, results from restricted transition-state shape selectivity, the very close dimensions of the pores and the PCP intermediates limit the reaction at the pore mouths along a rather small pore length. The constraint exerted by the narrow channels not only favours the formation of the less rigid ''end-PCP'' intermediate but also induces a slight deformation or distortion of the PCP ring in order to fit with the size of the pore. The PCP ring will be flattened to such an extent that the ring opening rate towards $2MeC_7$ is favoured. This picture explains adequately the observed product distributions of *n*-octane reaction over SAPO-11 and SAPO-41.

The conclusions that monobranched heptanes were formed inside the channels of SAPO-11 and SAPO-41 are further reinforced by the studies of branched C_8 isomers. While the activity of small and large crystal SAPO-11 samples differs only by a factor of 2 when 2,2,4 TMP is concerned, the activity of small crystal SAPO-11 is more than 10 times that of large crystal starting from monomethylheptanes. Similar observations were made starting from dimethyl hexanes. From the reaction of 2,2,4 TMP, it was concluded that the outer surface of large crystal SAPO-41 is almost inactive. By contrast, starting from methylheptanes, the activities of small and large crystal SAPO-41 samples differ only by a factor 2–3. The results indicate that the reaction of the methylheptanes must occur inside the intracrystalline voids at the pore mouths. Apparently pore-mouth catalysis over SAPO-41 is less important than over SAPO-11, since the change in the activity of small and large crystals in methylheptane reactions is less marked with SAPO-41. The product distributions starting from methylheptanes confirm the assumption that reactions occurred inside the channels at the pore mouths. It is well established for carbenium ion rearrangements that the reaction rates, where degree of branching does not change, are fast, while rearrangements, where degree of branching changes, are slow. Hence 1,2 methyl shift in monomethylalkyl carbenium ion is 4–5 times faster than PCP branching or debranching. In addition it has been demonstrated that methyl shift towards the centre of the carbon chain is faster than that towards the chain end. Hence starting from $2MeC_7$ one should expect a large excess of $3MeC_7$ with respect to *n*-C_8. The product distributions given in Table 4 shows in contrast that substantial amount of *n*-octane was formed over the four samples. The molecular ratio *n*-$C_8/3MeC_7$ was 0.32 and 0.54 , respectively, for large and small crystal SAPO-11, and 0.23 and 0.44, respectively, for large and small crystal SAPO-41. It is clear that the propensity for debranching of terminal methylheptanes increased as the pore dimensions decreases, SAPO-11 is more efficient than SAPO-41. Starting from $3MeC_7$ and $4MeC_7$ Table 4 shows that a relatively important fraction of *n*-octane was formed. This is also true starting from 2,4 and 2,5 $dMeC_6$.

Many experimental results have been brought to show that pore sizes and crystal sizes exert important influences upon the hydroisomerisation selectivity of SAPO-11 and SAPO-41. The shape-selective catalysis is referred to restricted transition-state shape selectivity at the pore mouths of the molecular sieves. This shape-selective catalysis is associated with the topology of the molecular sieves, the unidimensional shape of the channels in SAPO-11 and SAPO-41 restricts diffusion and counter diffusion of the molecules in the channels which allow only a fraction of the interior channel to participate in the reaction. Within the unidimensional small pores the reaction proceeds only in a single file. The bulky long-chain hydrocarbons would diffuse to only a short distance from the external surface boundary, and thus react at the so-called ''Pore Mouth''. It is also possible that only a part of the molecule enters the pore as suggested in [8]. However, pore mouth catalysis is also considered

when the entire molecule enters the pore as suggested in [11].

By decreasing the crystal size, the number of pore mouths participating in the reaction increases. The pore dimensions of SAPO-11 and SAPO-41 were too small to permit the formation of tribranched methyl carbenium ions inside the channels, thus prevents cracking reactions. High selectivity towards isomerisation results. In addition it appears that PCP intermediates can accommodate within the channels, particularly the less rigid end-cyclopropyl alkyl intermediate, the PCP cycle being more strongly distorted in the channels of the molecular sieves having the lowest dimensions, SAPO-11, for example. This configuration of the PCP intermediates favours ring opening into terminal methyl branched isomers. Product distributions from the reaction of 3-methylheptane illustrate nicely the scheme suggested above.

If $2MeC_7$ and $4MeC_7$ were formed by the classical 1,2 methyl shift, the amount of $4MeC_7$ would have been much larger than those indicated in Table 4. Hence one should conclude that within the pores of SAPO-11 and SAPO-41 the occurrence of 1,2 methyl shift is considerably hindered as compared with the occurrence of PCP intermediates and ring opening. One could suggest that the transition state involved in the mechanism of 1,2 methyl shift is bulkier than the PCP intermediate, the rate of its formation thus decreases to an extent which increases as the dimensions of the channels are smaller. The isomerisation involving the PCP intermediate is increased thus favouring methyl migration towards the end of the carbon chain.

The hypothesis that within SAPO-11 and SAPO-41, the major path for the isomerisation of methyl-branched C_8 isomers is through distorted PCP intermediates formed inside the channels supported by the large amount of $2MeC_7$ and n-C_8 formed from $3MeC_7$.

In conclusion, the mechanisms discussed in this work reinforces those already proposed in the literature, that is the hydroisomerisation of long chain alkanes requires that the reaction occurs inside narrow unidimensional pore system at the pore mouths. It is not necessary for the paraffins to enter deeply inside the pores.

References

[1] S. Ernst, J. Weitkamp, J.A. Martens, P.A. Jacobs, Appl. Catal. 48 (1989) 137.
[2] S.I. Miller, Microporous Mater. 2 (1994) 439.
[3] S.I. Miller, US Patent, 5 135 638 (1992).
[4] P. Mériaudeau, V.A. Tuan, V.T. Nghiem, S.Y. Lai, L.N. Hung, C. Naccache, J. Catal. 169 (1997) 55.
[5] P.A. Jacobs, J.A. Martens, J. Weitkamp, H.K. Beyer, Faraday Discuss. Chem. Soc. 72 (1982) 353.
[6] J.A. Martens, P.A. Jacobs, Zeolites 6 (1986) 334.
[7] J.A. Martens, R. Parton, L. Uytterhoeven, P.A. Jacobs, Appl. Catal. 76 (1991) 95.
[8] J.A. Martens, W. Souverijns, W. Verrelst, G.F. Froment, P.A. Jacobs, Angew. Chem., Int. Ed. Engl. 34 (1995) 2528.
[9] S.T. Wilson, B.M. Lok, E.M. Flaningen, US Patent, 4 310 440 (1982).
[10] B.M. Lok, C.A. Messina, R.I. Patton, R.T. Gajek, T.R. Cannan, E.M. Flaningen, US Patent, 4 440 871 (1984).
[11] P. Mériaudeau, Vu A. Tuan, F. Lefebvre, Vu T. Nghiem, C. Naccache, Microporous Mater. (1998), submitted for publication.